

Local Normalization Distortion and the Thermodynamic Formalism of Decoding Strategies for Large Language Models

Tom Kempton^{1,*}, Stuart Burrell^{2,*}

¹Department of Mathematics, University of Manchester

²Innovation Lab, Featurespace

Correspondence: thomas.kempton@manchester.ac.uk

Abstract

Advances in hardware and language model architecture have spurred a revolution in natural language generation. However, autoregressive models compute probability distributions over next-token choices, and sampling from these distributions, known as decoding, has received significantly less attention than other design choices. Existing decoding strategies are largely based on heuristics, resulting in methods that are hard to apply or improve in a principled manner. We develop the theory of decoding strategies for language models by expressing popular decoding algorithms as equilibrium states in the language of ergodic theory and stating the functions they optimize. Using this, we analyze the effect of the local normalization step of top-k, nucleus, and temperature sampling, used to make probabilities sum to one. We argue that local normalization distortion is a fundamental defect of decoding strategies and quantify the size of this distortion and its effect on mathematical proxies for the quality and diversity of generated text. Contrary to the prevailing explanation, we argue that the major cause of the under-performance of top-k sampling relative to nucleus sampling is local normalization distortion. This yields conclusions for the future design of decoding algorithms and the detection of machine-generated text.

1 Introduction

Autoregressive large-language models are poised to transform industries such as healthcare, finance and education (Zhao et al., 2024). Rapid advancements in this field have been fueled by scaling (Hoffmann et al., 2024), transformer network architectures (Vaswani et al., 2017), and alignment processes (Christiano et al., 2017; Rafailov et al., 2024). However, autoregressive language models produce conditional *distributions* over predicted

next tokens, and these must be iteratively sampled during inference. A suite of *decoding* methods exist for this sampling, such as top k, nucleus, or temperature sampling, but these are based on heuristics and our understanding of these methods is in its infancy, with most being developed through trial and error (Wiher et al., 2022).

This is surprising since the choice of decoding strategy has a profound impact on the quality of the generated text and, in some cases, may be more important than the model architecture (Wiher et al., 2022). For example, greedy sampling, or the related concept of beam search, tends to produce accurate but repetitive or dull text (Holtzman et al., 2020). In contrast, pure sampling produces much more varied and interesting text but can produce text which is ‘incoherent and almost unrelated to the context’ (Holtzman et al., 2020).

Our primary goal is to fill this gap and initiate the theoretical study of decoding strategies. As an application of this theory, we investigate a well-known defect of popular decoding strategies, which results from truncating the distribution of possible next tokens at each step during inference. Truncation necessitates repeated renormalization to obtain valid probability distributions, and results in a phenomenon we term *local normalization distortion*. The fact that local normalization distorts the resulting probability distribution is well-known, but not well-understood. Local normalization distortion measures deviation from the learned conditional distributions of a language model, and we theoretically and empirically validate claims on its relationship to the quality of generated text. In summary, our contributions are as follows.

1. Develop a theoretical framework for analyzing decoding strategies. This involves describing the probability distributions q produced by decoding algorithms as equilibrium states, drawing heavily on the language of er-

*Equal contribution.

godic theory and thermodynamic formalism (Bowen, 2008). We precisely state the function maximized by each decoding strategy; see Section 5.

- Quantify the effect of local normalization distortion by showing how the probability of randomly chosen strings change when we replace a locally normalized decoding strategy with a globally normalized equivalent. The effect is large for top-k and temperature sampling, but much smaller for nucleus sampling; see Section 6.1.
- Evaluate language models and decoding strategies in terms of a quality-diversity trade-off, as in Caccia et al. (2019). We show, both theoretically and empirically, that local normalization distortion negatively affects the performance of the decoding strategy. Indeed, we show that the widely noted quality-diversity under-performance of top-k sampling relative to nucleus (top-p) sampling can be entirely explained by local normalization distortion.

These results show that in the ongoing search for better decoding strategies for large language models, careful attention should be paid to local normalization distortion, as it has a large effect on the quality of generated text, and the size of this effect varies considerably with choice of decoding strategy. In a follow-up article, we also show how one can use local normalization distortion to detect machine-generated text.

Before diving into the technical details, it is best to first motivate the theory with a simple illustration.

2 Motivating Example

Many autoregressive models for natural language generation work broadly as follows. Given a vocabulary \mathcal{V} , one builds a large neural network to estimate the likelihood $p(y_t | \mathbf{y}_{<t})$ that the next token in a sequence is equal to $y_t \in \mathcal{V}$, given the previous tokens $\mathbf{y}_{<t} = y_0 \cdots y_{t-1} \in \mathcal{V}^t$. Then, one decides on a decoding strategy (sampling algorithm), which is a way of using the collection of likelihoods

$$\{p(y_t | \mathbf{y}_{<t}) : y_t \in \mathcal{V}\}$$

associated with context $\mathbf{y}_{<t}$ to choose the next token y_t . For example, one could always choose the

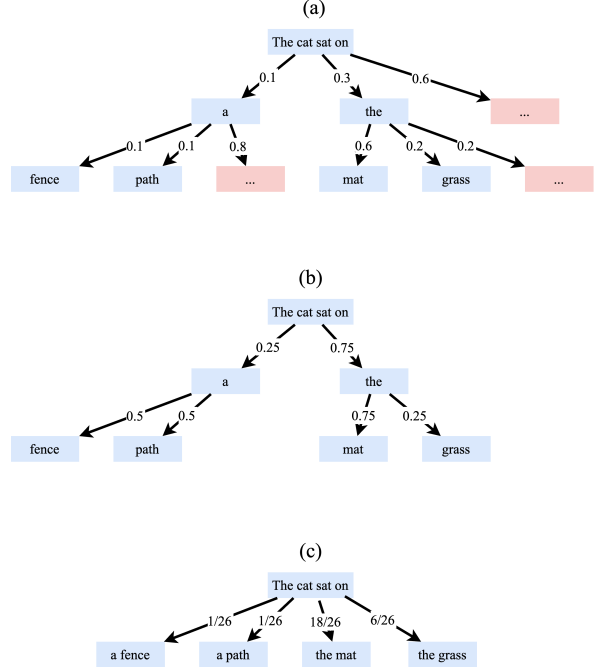


Figure 1: Distortion due to local normalization significantly impacts the implied probability distribution during decoding. (a) shows pure sampling, (b) shows locally normalized sampling, and (c) shows globally normalized sampling.

token y_t which has highest likelihood $p(y_t | \mathbf{y}_{<t})$ (greedy sampling), or one could allow each token y_t to be chosen with probability equal to the likelihood $p(y_t | \mathbf{y}_{<t})$ (pure sampling). Let $q(\cdot | \mathbf{y}_{<t})$ denote the distribution of choices of y_t given the context and chosen decoding strategy.

Finally, having chosen the token y_t , one repeats the process to choose y_{t+1} given the new context $\mathbf{y}_{<t+1}$. One computes the probability of a string $y_0 \cdots y_T \in \mathcal{V}^*$ by

$$q(y_0 \cdots y_T) = \prod_{t=1}^T q(y_t | \mathbf{y}_{<t}).$$

In many settings, rather than conditioning on the whole history $\mathbf{y}_{<t}$ one allows only a finite context length L and conditions on $y_{t-L} \cdots y_{t-1}$, making the process of generating texts an L -step Markov process.

A simple example shows how the decoding strategy can dramatically influence q . Suppose we have a language model that produces model likelihoods p . We feed in the context ‘The cat sat on’ and obtain the likelihoods of the various choices of the next two tokens. Let these likelihoods be as described in Figure 1. Assume further that we decide that various choices of tokens are unreliable and

so we wish to restrict our choices to the two most likely tokens depicted in blue boxes. We now have probabilities which do not sum to one, and so have to decide how to normalize them.

Option 1: Global normalization Compute the probabilities of complete strings and divide by the sum of the probabilities of complete strings. In our example, the sum of the probabilities of complete strings is $0.26 = 0.01 + 0.01 + 0.18 + 0.06$. We end up with ‘The cat sat on a fence’ being selected with probability $0.01/0.26 \approx 0.038$.

Option 2: Local normalization Renormalize conditional probabilities locally so that the probabilities of outward edges from each node sum to one. For example, we choose first word ‘a’ with probability $0.1/0.4$ and ‘the’ with probability $0.3/0.4$. With local normalization, we end up with ‘The cat sat on a fence’ being selected with probability $0.25 \times 0.5 = 0.125$.

We see that these two different methods of normalizing probabilities yield very different probability distributions. Figure 1 uses a decoding strategy that considers the two most likely tokens at each step, known as top-k sampling with $k = 2$. In the next section we formally define the array of decoding strategies we study in this article and that are used in common practice.

3 Decoding Strategies

The decoding strategies we study in this article fall into two classes, truncation sampling algorithms (such as nucleus sampling and top-k) and temperature sampling. Truncation sampling algorithms work by defining an allowed set $\mathcal{A}_{\mathbf{y}_{<t}}$ of tokens that can follow some context, restricting the model conditional probability distribution $p(\cdot|\mathbf{y}_{<t})$ to this set and renormalizing it to have mass one.

Definition 3.1 (Truncation Sampling Algorithms). *Given a language model p , a context $\mathbf{y}_{<t}$ and an allowed set $\mathcal{A}_{\mathbf{y}_{<t}}$, define*

$$Z(\mathbf{y}_{<t}) = \sum_{w_t \in \mathcal{A}_{\mathbf{y}_{<t}}} p(w_t|\mathbf{y}_{<t}).$$

Choose element y_t of $\mathcal{A}_{\mathbf{y}_{<t}}$ with probability

$$q(y_t|\mathbf{y}_{<t}) := \frac{p(y_t|\mathbf{y}_{<t})}{Z(\mathbf{y}_{<t})}$$

and set

$$q(y_t|\mathbf{y}_{<t}) = 0$$

for $y_t \notin \mathcal{A}_{\mathbf{y}_{<t}}$.

Top-k sampling (Fan et al., 2018) is an example of a truncation sampling strategy. Given some value of $k \geq 1$, it is defined by setting the allowed set $\mathcal{A}_{\mathbf{y}_{<t}}$ to be the set of those k tokens with highest model probabilities $p(y_t|\mathbf{y}_{<t})$. Top-k sampling restricts to the k most likely tokens at each stage of language generation, and renormalizes mass at each stage of generation by dividing model probabilities by the sum of the probabilities of the top-k tokens.

Nucleus (top-p) sampling (Holtzman et al., 2020) is defined by choosing a value $\pi \in [0, 1]$, ordering tokens $w_1, w_2, \dots \in \mathcal{V}$ in order of decreasing model probability $p(w_i|\mathbf{y}_{<t})$ and setting $\mathcal{A}_{\mathbf{y}_{<t}} = \{w_1, \dots, w_r\}$ where the threshold r is the smallest natural number satisfying $\sum_{i=1}^r p(w_i|\mathbf{y}_{<t}) \geq \pi$. Rather than choosing from exactly k tokens at each stage, nucleus sampling samples from (roughly) the top proportion π of the probability distribution. It is worth stressing that $\sum_{i=1}^r p(w_i|\mathbf{y}_{<t})$ is often much larger than π , and so the normalizing constant $Z(\mathbf{y}_{<t}) = \sum_{i=1}^r p(w_i|\mathbf{y}_{<t})$ can vary significantly at different contexts.

Several newer truncation-based decoding strategies have been introduced with different (and rather clever) ways of choosing the allowed sets $\mathcal{A}_{\mathbf{y}_{<t}}$, see, for example, locally typical sampling (Meister et al., 2023), η -sampling (Hewitt et al., 2022) and microstat (Basu et al., 2020). One observation about this body of research is that careful motivation is always given for the choice of allowed set, but little if any consideration is given to the way in which the resulting decoding strategy apportions probability mass within this allowed set.

Finally, we mention temperature sampling, which is the only widely used stochastic sampling algorithm not to fall into the framework of truncation sampling.

Definition 3.2 (Temperature Sampling (Guo et al., 2017)). *Given some context $\mathbf{y}_{<t}$ and a parameter $\tau > 0$ (usually $\tau \in (0, 1)$), define*

$$Z_\tau(\mathbf{y}_{<t}) = \sum_{w_t \in \mathcal{V}} (p(w_t|\mathbf{y}_{<t}))^{\frac{1}{\tau}}.$$

The distribution q_τ given by temperature sampling is defined by

$$q_\tau(y_t|\mathbf{y}_{<t}) = \frac{p(y_t|\mathbf{y}_{<t})^{\frac{1}{\tau}}}{Z_\tau(\mathbf{y}_{<t})}.$$

3.1 Global Normalization

As in our toy example, we could replace the local normalization in top-k, nucleus and temperature sampling with a global normalization, in which rather than normalizing conditional probabilities by dividing by $Z(\mathbf{y}_{< \mathbf{m}+i})$ at each step, one normalizes the joint distribution over complete sequences $w_1 \cdots w_T$. For example, if we let \mathcal{A}_T denote the set of sequences of length T for which each token is in the top-k set, globally normalized top-k sampling selects string $y_1 \cdots y_T \in \mathcal{A}_T$ with probability

$$q'_k(y_1 \cdots y_T) = \frac{p(y_1 \cdots y_T)}{\sum_{w_1 \cdots w_T \in \mathcal{A}_T} p(w_1 \cdots w_T)}. \quad (1)$$

That is, globally normalized top-k sampling samples according to the measure p conditioned on the subset \mathcal{A}_T . Similar statements hold for globally normalized variants of any restriction sampling algorithm. Globally normalized temperature sampling selects tokens with probability proportional to $p(\cdot | \mathbf{y}_{< \mathbf{t}})^{\frac{1}{\tau}}$, as is the case when temperature is used in statistical physics, ergodic theory and fractal geometry (see Appendix C).

We let q'_k , q'_π and q'_τ denote the globally normalized alternatives to top-k, nucleus and temperature sampling respectively. Globally normalized decoding strategies are computationally infeasible, even for fairly small values of T . We introduce them here as a theoretical tool to better understand how problematic local normalization distortion is. In Appendix B we explain how to sample from q'_k , q'_π and q'_τ using rejection sampling.

3.2 Local Normalization Distortion

Definition 3.3. *Let q be the distribution produced by a locally normalized decoding strategy, and let q' be its globally normalized counterpart. Given a context $\mathbf{y}_{< \mathbf{t}}$, the local normalization distortion associated to completion $y_t \cdots y_T$ is defined as*

$$\frac{q(y_t \cdots y_T | \mathbf{y}_{< \mathbf{t}})}{q'(y_t \cdots y_T | \mathbf{y}_{< \mathbf{t}})}.$$

In the case of top-k sampling, given context $\mathbf{y}_{< \mathbf{t}}$, there is a constant C such that each completion $y_t \cdots y_T$ has local normalization distortion

$$\frac{1}{C} \cdot \frac{1}{\prod_{i=0}^{T-t} Z_k(\mathbf{y}_{< \mathbf{t}+i})},$$

where Z_k is the mass of the top-k tokens at context $\mathbf{y}_{< \mathbf{t}+i}$. The constant C is the normalizing constant

associated to global normalization, which is hard to compute but can be bypassed in empirical investigations, see Section 6.

We conclude this section with a proposition that further motivates the study of local normalization distortion.

Proposition 3.1. *Let p be a language model, q_τ denote the distribution arising from temperature sampling, and q'_τ the distribution arising from a globally normalized version of temperature sampling. Then, as the temperature parameter τ tends to zero, q_τ converges to the distribution putting all of its mass on the output of greedy sampling, whereas q'_τ converges to the distribution putting all of its mass on the sequence with globally maximal log probability.*

Proof. See Appendix D.1. □

Given the substantial interest in implementing expensive search algorithms such as beam search to find sequences with approximately the globally maximal log probability, we present this example as initial evidence that local normalization distortion can have a substantial negative effect and is worthy of further investigation.

4 Evaluating Decoding Strategies through a Quality-Diversity Trade Off

When generating text from a language model, one may have different preferences for the ‘quality’ and ‘diversity’ of the text according to the task being performed (such as machine translation, or short story generation) (Caccia et al., 2019; Wiher et al., 2022). Selecting only tokens with high likelihood produces accurate but dull text, whereas sampling from the whole distribution allows for more varied text at the risk of losing coherence. Thus, the choice of sampling algorithm affects the balance between the quality and diversity of generated text. This framing of choice of decoding strategy choice as a trade-off of quality and diversity is studied in Caccia et al. (2019); Ippolito et al. (2019); Nadeem et al. (2020); Zhang et al. (2021). In particular, in Caccia et al. (2019), the authors propose using a ‘temperature sweep’ to find a parameter τ for which temperature sampling best matches this preference. Similarly, one can adjust the parameters in top-k or nucleus sampling according to one’s preferences for diversity versus quality, since restricting token choices to the top of the distribution prioritizes quality over diversity.

There are no universally accepted definitions of the diversity and quality of text. One way of evaluating the diversity of stochastically generated text is to look at the entropy $H(q)$ of the distribution q of the text, given by

$$H(q) = \sum_{\mathbf{y} \in \mathcal{V}^*} q(\mathbf{y}) \log q(\mathbf{y}).$$

The sum here is taken over complete strings.

The gold standard for evaluating the quality of the generated text is to get human judgment scores, although this is expensive and fraught with difficulty (Clark et al., 2021). Often the model log-likelihood $\log(p)$ is used as a proxy for quality, so the quality of a distribution q over possible texts would be given by

$$Q(q) = \sum_{\mathbf{y} \in \mathcal{V}^*} q(\mathbf{y}) \log p(\mathbf{y}).$$

This notion of quality is not without its issues (Meister et al., 2022), although Zhang et al. (2021) has a rather compelling graph suggesting that human judgements of quality of text are very well correlated with a continuous function of $Q(q)$.

While entropy and average log-likelihood of a distribution q are imperfect, albeit frequently used, proxies for diversity and quality, they are precisely the right objects to describe mathematically the quantities maximized by the distributions resulting from top-k sampling, nucleus sampling and temperature sampling.

5 Decoding Strategies as Equilibrium States

In the last section we reviewed the literature on what a decoding strategy ought to maximize. In this section we prove results about what popular decoding strategies actually optimize. In particular, we state results of the form ‘given some context $\mathbf{y}_{< \mathbf{m}}$, the probability distribution q on the set $\mathcal{A}_{\mathbf{y}_{< \mathbf{m}}, k}^*$ obtained by sampling according to a certain decoding strategy is the unique probability distribution on $\mathcal{A}_{\mathbf{y}_{< \mathbf{m}}, k}^*$ which maximizes the following function...’.

In the language of ergodic theory, what we are doing is describing the outcome of a decoding strategy as an *equilibrium state* associated to a certain potential. While the mathematics of this section is not hard, it is useful as it allows us to ask whether the function that our decoding strategy maximizes

is well aligned with the theoretical goals of a decoding strategy. In a follow-up paper we use the results of this section to theoretically justify a method of detecting language model generated text.

We use the following standard result. As usual, let $0 \log 0 := 0$.

Lemma 5.1 ((Bowen, 2008), Lemma 1.1). *Let $X = \{1, \dots, k\}$ be a finite set and let $R = (r_1, \dots, r_k)$ be a probability measure on X assigning mass r_i to symbol i . Then R is the unique probability measure maximizing the quantity*

$$\underbrace{- \sum_{i \in X} \mu_i \log \mu_i}_{\text{Entropy } H(\mu)} + \underbrace{\sum_{i \in X} \mu_i \log r_i}_{\text{Average log probability}}$$

among probability measures $\mu = (\mu_1, \dots, \mu_k)$ on X .

The results of this section follow as direct corollaries to Lemma 5.1 by analyzing the measures (r_1, \dots, r_k) given by various decoding strategies. Details are given in the appendix D. Our first result concerns top-k decoding.

Corollary 5.1. *Given some context $\mathbf{y}_{< \mathbf{m}}$ and a choice of k , the distribution q_k on $\mathcal{A}_{\mathbf{y}_{< \mathbf{m}}, k}^*$ produced by top-k sampling is the unique distribution maximizing the quantity*

$$\begin{aligned} & \underbrace{H(\mu)}_{\text{Proxy for diversity}} \\ & + \underbrace{\sum_{\mathbf{w} \in \mathcal{A}_{\mathbf{y}_{< \mathbf{m}}, k}^*} \mu(\mathbf{w} | \mathbf{y}_{< \mathbf{m}}) \log p(\mathbf{w} | \mathbf{y}_{< \mathbf{m}})}_{\text{Proxy for quality}} \\ & + \underbrace{\sum_{\mathbf{w} \in \mathcal{A}_{\mathbf{y}_{< \mathbf{m}}, k}^*} \mu(\mathbf{w} | \mathbf{y}_{< \mathbf{m}}) \log \epsilon_k(\mathbf{w})}_{\text{Distortion term}} \end{aligned}$$

among distributions μ on $\mathcal{A}_{\mathbf{y}_{< \mathbf{m}}, k}^*$. Here

$$\epsilon_k(\mathbf{w}) := \frac{1}{\prod_{i=0}^{T-m} Z(y_0 \dots y_m w_{m+1} \dots w_{m+i-1})}.$$

which is the product along the sequence of the inverse of the mass of the top k tokens.

If our equation above had only the first two terms, it would show that q_k maximizes the sum of mathematical proxies for diversity and quality among distributions supported on $\mathcal{A}_{\mathbf{y}_{< \mathbf{m}}, k}^*$. The third term however, which is an artifact of local normalization, distorts this goal. If the third term was constant

across sequences \mathbf{y} then it would have no effect, but issues arise when it has a large variance; see Section 6.1. Next, we consider nucleus sampling.

Corollary 5.2. *Given some context $\mathbf{y}_{<\mathbf{m}}$ and a choice of π , the distribution q_π on $\mathcal{A}_{\mathbf{y}_{<\mathbf{m}},\pi}^*$ generated by nucleus sampling is the unique distribution maximizing the quantity*

$$H(\mu) + \sum_{\mathbf{w} \in \mathcal{A}_{\mathbf{y}_{<\mathbf{m}},\pi}^*} \mu(\mathbf{w}|\mathbf{y}_{<\mathbf{m}}) \log p(\mathbf{w}|\mathbf{y}_{<\mathbf{m}}) + \sum_{\mathbf{w} \in \mathcal{A}_{\mathbf{y}_{<\mathbf{m}},\pi}^*} \mu(\mathbf{w}|\mathbf{y}_{<\mathbf{m}}) \log \epsilon_\pi(\mathbf{w})$$

among distributions μ on $\mathcal{A}_{\mathbf{y}_{<\mathbf{m}},\pi}^*$. Here

$$\epsilon_\pi(\mathbf{w}) := \frac{1}{\prod_{i=0}^{T-m} Z(y_0 \cdots y_m w_{m+1} \cdots w_{m+i-1})}$$

which is the inverse of the product along the sequence $w_{m+1} \cdots w_T$ of the total mass of those tokens allowed by nucleus sampling.

Thus nucleus sampling produces a distribution q_π maximizing a goal related to quality, diversity and an error term related to both by the length of the sequence y and the extent to which the mass of the tokens selected by nucleus sampling overshoots the target π .

Finally, we consider temperature sampling.

Corollary 5.3. *Given some choice of temperature τ and context $\mathbf{y}_{<\mathbf{m}}$, the distribution q_τ is the distribution maximizing the quantity*

$$H(\mu) + \frac{1}{\tau} \sum_{\mathbf{w} \in \mathcal{V}^*} \mu(y_1 \cdots y_m \mathbf{w}) \log(p(y_1 \cdots y_m \mathbf{w})) + \sum_{\mathbf{w} \in \mathcal{V}^*} \mu(y_1 \cdots y_m \mathbf{w}) \epsilon_\tau(\mathbf{w})$$

among distributions μ on \mathcal{V}^* , where

$$\epsilon_\tau(\mathbf{w}) = \frac{1}{\prod_{i=0}^{T-m} Z_\tau(y_0 \cdots y_m w_{m+1} \cdots w_{m+i-1})}$$

When nucleus or top-k sampling set $\pi < 1$ or $k < |\mathcal{V}|$, they produce distributions with lower entropy than p , since token choice has been reduced. This process also redistributes mass from low probability tokens to higher probability tokens, reducing the average log likelihood. Thus the parameters associated with nucleus or top-k sampling allow one to prioritize quality or diversity. This is somewhat hidden in the statements of Corollaries 5.1 and 5.2, it appears only in that it is the space of distributions

on \mathcal{A}^* upon which the proxy for diversity, proxy for quality, and distortion term are maximized.

Temperature sampling is not a truncation algorithm, and the way it modulates between prioritizing quality and prioritizing diversity is in the factor $1/\tau$ preceding the mathematical proxy for quality in the main equation of Corollary 5.3. As before, the third term here is not related to the goal of maximizing quality or diversity. It is broadly similar to the distortion introduced by top-k, except rather than dividing by the product along a sequence of the mass contained in the top-k tokens, it divides by the product along a sequence $y_m \cdots y_T$ of the $L_{1/\tau}$ norm of the distribution $p(\cdot|\mathbf{y}_{<\mathbf{m}+i})$.

Finally, we see that global normalization removes the problematic third term in each of the quantities maximized by our decoding strategies.

Corollary 5.4. *In each of corollaries 5.1-5.3, if the locally normalized probability distribution (q_k , q_π , or q_τ) is replaced by its globally normalized equivalent, the statement of the theorem remains the same except without the third term (i.e. the distortion term) in the expression for the maximized quantity.*

This is important because it shows that, in terms of the quality-diversity trade off goals of the previous section, locally normalized decoding strategies perform strictly worse than their globally normalized counterparts. In Section 6.2 we quantify this effect.

6 Experiments

All of our experiments are run using Llama 2-7B (Touvron et al., 2023) on a single A100 GPU. Detailed setup for each experiment is contained in the corresponding sections and appendices.

The primary challenge to running these experiments is the computational cost of global normalization. To do this efficiently, we introduce a process based on rejection sampling in Appendix B. It is revealing that, while these computational limitations mean some experiments may only be feasibly run on short passages of generated text, this is sufficient to reliably observe that the effects predicted by our theory do indeed hold in practice.

6.1 How Large is the Distortion due to Local Normalization under Different Decoding Strategies?

In assessing how much local normalization distortion affects the mass of a completion $y_m \cdots y_T$, we

need to compare how much $q(y_m \cdots y_T | \mathbf{y}_{< \mathbf{m}})$ is boosted by local normalization against how much it would have been boosted by global normalization, as in Definition 3.3. Considering, for example, top-k sampling, if q_k denotes the distribution produced by top-k sampling and q'_k denotes its globally normalized equivalent, we would like to compute

$$\frac{q_k(y_m \cdots y_T | \mathbf{y}_{< \mathbf{m}})}{q'_k(y_m \cdots y_T | \mathbf{y}_{< \mathbf{m}})}.$$

This is difficult to compute because globally normalized top-k assigns mass

$$q'_k(y_m \cdots y_T | \mathbf{y}_{< \mathbf{m}}) = \frac{p(y_m \cdots y_T | \mathbf{y}_{< \mathbf{m}})}{C}$$

for some constant C , which is very expensive to compute, particularly on long generations. Instead, we generate pairs of completions $y_m \cdots y_T$ and $z_m \cdots z_T$ by top-k sampling and then compute the ratio of the two local normalization distortions by computing

$$\frac{q_k(y_m \cdots y_T | \mathbf{y}_{< \mathbf{m}})}{q'_k(y_m \cdots y_T | \mathbf{y}_{< \mathbf{m}})} / \frac{q_k(z_m \cdots z_T | \mathbf{y}_{< \mathbf{m}})}{q'_k(z_m \cdots z_T | \mathbf{y}_{< \mathbf{m}})} \quad (2)$$

which is equal to

$$\frac{q_k(y_m \cdots y_T | \mathbf{y}_{< \mathbf{m}})}{p(y_m \cdots y_T | \mathbf{y}_{< \mathbf{m}})} \cdot \frac{p(z_m \cdots z_T | \mathbf{y}_{< \mathbf{m}})}{q_k(z_m \cdots z_T | \mathbf{y}_{< \mathbf{m}})}. \quad (3)$$

Since we are taking the ratio of the two local normalization distortions, the global constants C cancel out and so do not need computing.

For $k = 5, 50, 150$, we start by finding values of π and τ such that on average, for a randomly chosen context, $Z_k(\mathbf{y}_{< \mathbf{t}}) \approx Z_\pi(\mathbf{y}_{< \mathbf{t}}) \approx Z_\tau(\mathbf{y}_{< \mathbf{t}})$. We are seeking here to tune our parameters so that the average amount of renormalizing done by top-k, nucleus and temperature sampling is the same.

Having tuned parameters, we then compare the local normalization distortion across the three decoding strategies. Starting with the single word context ‘The’, we generate 1000 pairs of completions of 100 tokens each for each of our decoding strategies and parameter choices. We compute the relative local normalization distortion given by the quantity (3) for top-k sampling and equivalent quantities for nucleus and temperature sampling, see Appendix A.

Our results are presented in Figure 3 and Table 1. We have two key findings.

Table 1: Local normalization distortion ratios over a range of comparable decoding strategies. The table is partitioned into three groups of parameters tuned so that the average amount of renormalization is equal. Reported quantiles are the absolute value of the natural log of the ratio (2).

Decoding Strategy	Quantile				
	10%	25%	50%	75%	90%
$k = 5$	1.53	3.87	8.63	14.72	20.84
$\tau = 0.91$	0.95	2.00	4.30	7.44	10.54
$p = 0.77$	0.35	1.01	2.39	4.14	6.03
$k = 50$	0.72	1.72	3.30	5.43	8.15
$\tau = 0.95$	0.47	1.11	2.44	4.01	5.74
$p = 0.88$	0.19	0.51	1.07	1.85	2.80
$k = 150$	0.34	0.97	2.02	3.50	4.97
$\tau = 0.99$	0.08	0.23	0.49	0.83	1.27
$p = 0.96$	0.06	0.13	0.27	0.47	0.70

Finding 1: Local normalization distortion has a large effect. For example, when using temperature sampling with parameter $\tau = 0.91$ to sample pairs of sequences \mathbf{w}, \mathbf{z} , each of length 100, we see that in half of cases, the ratio $q_\tau(\mathbf{w}|\mathbf{c})/q_\tau(\mathbf{z}|\mathbf{c})$ differs from the ratio $p(\mathbf{w}|\mathbf{c})^{1/\tau}/p(\mathbf{z}|\mathbf{c})^{1/\tau}$ by a factor of at least $\exp(4.3) \approx 74$. That is, the effect of local normalization distortion is to distort the relative probabilities of two completions by a factor of 74.

It is worth stressing that temperature sampling is more often used with temperatures 0.7 or 0.8, in which case one would see even larger local normalization distortion.

Finding 2: When parameters k, τ and π are tuned so that the typical renormalization factors Z_k, Z_τ and Z_π are similar, nucleus sampling results in a much smaller local normalization distortion than temperature sampling, which in turn gives rise to a much smaller distortion than top-k sampling.

6.2 How does Local Normalization Distortion affect the Quality-Diversity Trade Off?

Given a single word context $w_1 = \text{‘The’}$, we generate length 15 samples by top-k sampling, nucleus sampling, temperature sampling and their globally normalized equivalents. We do this over a range of values of k, π and τ . For each sample $w_2 \cdots w_{16}$, we assess the quality by computing the negative log probability $-\log(p(w_2 \cdots w_{16} | w_1))$. In addition, we evaluate the diversity of our sample generation process by approximating the entropy of our

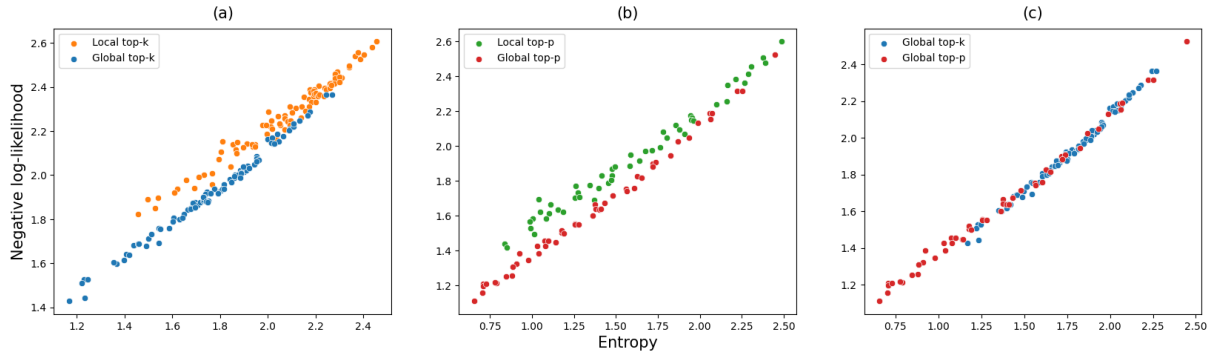


Figure 2: Evaluating quality against diversity at different parameter values when decoding with top-k, nucleus sampling and globally normalized top-k. The ranges were $k = 10, 11, \dots, 100$ and $p = 0.4, 0.41, \dots, 0.9$. Higher values of entropy are better, lower values of negative-log-likelihood are better.

generation process using the Shannon-McMillan-Breimann theorem (Walters, 2000). That is, for each choice of decoding strategy and parameter value and each completion $w_2 \cdots w_{16}$ generated by decoding strategy q , we compute $-\log(q(w_2 \cdots w_{16}|w_1))$. We average these values over the different completions generated for each particular decoding strategy and parameter value to approximate $H(q)$. Figure 2 shows these proxies for quality and diversity. Note that lower negative log probability and higher entropy are preferable.

Finding 3: For both top-k and nucleus sampling, globally normalized sampling outperforms locally normalized sampling on the quality-diversity trade off. That is, at any fixed value of entropy, globally normalized sampling produces texts with higher log likelihood.

Finding 4: As noted in Caccia et al. (2019), (locally normalized) top-k sampling performs worse than nucleus sampling on the quality-diversity trade off. However, when each sampling strategy is replaced with its globally normalized variant, the two methods perform equally well. Thus, the under-performance of top-k sampling relative to nucleus sampling is entirely explained by local normalization distortion.

It is not tractable to compute globally normalized temperature sampling for sensible ranges of τ , due to the extreme rejection rate of our rejection sampling algorithm. Fortunately, we do not require experimental results in this setting thanks to Corollary 5.4, which states that globally normalized temperature sampling at temperature τ yields the unique distribution maximizing entropy plus $1/\tau$ log-likelihood among measures on \mathcal{A}^T .

7 Conclusions

By expressing popular decoding strategies as equilibrium states, one can see that the quantity which they maximize contains a term relating to local normalization of probability mass which seems unrelated to any reasonable goal of a decoding strategy. In particular, this term pulls the resulting probability distribution away from the quality-diversity maximizing curve. We have shown experimentally that the effect of local normalization distortion on the probability of selecting a string is typically very large (Section 6.1), and that it has a strongly negative effect on the quality-diversity tradeoff (Section 6.2). This accounts for the under-performance of top-k sampling relative to nucleus sampling on this metric. All of these factors lead us to the conclusion that local normalization distortion has a profoundly negative effect on machine-generated text and that it should be carefully considered both when practitioners choose a decoding strategy and in the design of future methods.

8 Ethical Considerations

This work considers current decoding strategies for language models and ways in which these decoding strategies fall short. The most likely practical applications of it are in the detection of machine-generated text and in improving language models so as to make their outputs more human-like.

Although there are no specific ethical concerns about this work, we do inherit wider ethical questions around building human-like language models and detecting machine-generated text. A discussion of these is far beyond the scope of this work; instead, we encourage the reader to seek out the wealth of publicly available material on the issues.

9 Limitations

Our experiments are run on the open-source Llama 2 language model. While this is not uncommon for research in computational linguistics, the setting in which decoding strategies such as temperature sampling are most widely deployed is in closed-source models such as ChatGPT (OpenAI, 2022). Our theoretical results hold for all language models and we do not believe the conclusions of our experimental section would change with language model. It is however the case that the magnitude of local normalization distortion would decrease if the entropies of the next token probability distributions were typically lower. Thus, language models with higher certainty about their next token predictions would give rise to smaller numbers in Table 1, for example.

We have used log-likelihood as a proxy for the quality of machine-generated text and entropy as a proxy for its diversity. These metrics are clearly imperfect. In particular, human judgement of text quality may be a better metric for the quality of a text, although obtaining these human judgements often prohibitive due to cost (Clark et al., 2021).

References

- Sourya Basu, Govardana Sachitanandam Ramachandran, Nitish Shirish Keskar, and Lav R Varshney. 2020. Mirostat: A neural text decoding algorithm that directly controls perplexity. In *International Conference on Learning Representations*.
- Robert Edward Bowen. 2008. *Equilibrium states and the ergodic theory of Anosov diffeomorphisms*, volume 470. Springer Science & Business Media.
- Julien Brémont. 2002. Gibbs measures at temperature zero. *Nonlinearity*, 16(2):419.
- Massimo Caccia, Lucas Caccia, William Fedus, Hugo Larochelle, Joelle Pineau, and Laurent Charlin. 2019. Language gans falling short. In *International Conference on Learning Representations*.
- Paul F. Christiano, Jan Leike, Tom B. Brown, Miljan Martic, Shane Legg, and Dario Amodei. 2017. Deep reinforcement learning from human preferences. In *Proceedings of the 31st International Conference on Neural Information Processing Systems, NIPS’17*, page 4302–4310, Red Hook, NY, USA. Curran Associates Inc.
- Elizabeth Clark, Tal August, Sofia Serrano, Nikita Haduong, Suchin Gururangan, and Noah A Smith. 2021. All that’s ‘human’ is not gold: Evaluating human evaluation of generated text. In *Proceedings of the 59th Annual Meeting of the Association for Computational Linguistics and the 11th International Joint Conference on Natural Language Processing (Volume 1: Long Papers)*, pages 7282–7296.
- Kenneth Falconer. 2007. *Fractal geometry: mathematical foundations and applications*. John Wiley & Sons.
- Angela Fan, Mike Lewis, and Yann Dauphin. 2018. Hierarchical neural story generation. In *Proceedings of the 56th Annual Meeting of the Association for Computational Linguistics (Volume 1: Long Papers)*. Association for Computational Linguistics.
- Chuan Guo, Geoff Pleiss, Yu Sun, and Kilian Q Weinberger. 2017. On calibration of modern neural networks. In *International conference on machine learning*, pages 1321–1330. PMLR.
- John Hewitt, Christopher D Manning, and Percy Liang. 2022. Truncation sampling as language model desmoothing. In *Findings of the Association for Computational Linguistics: EMNLP 2022*, pages 3414–3427.
- Jordan Hoffmann, Sebastian Borgeaud, Arthur Mensch, Elena Buchatskaya, Trevor Cai, Eliza Rutherford, Diego de Las Casas, Lisa Anne Hendricks, Johannes Welbl, Aidan Clark, Tom Hennigan, Eric Noland, Katie Millican, George van den Driessche, Bogdan Damoc, Aurelia Guy, Simon Osindero, Karen Simonyan, Erich Elsen, Oriol Vinyals, Jack W. Rae, and Laurent Sifre. 2024. Training compute-optimal large language models. In *Proceedings of the 36th International Conference on Neural Information Processing Systems, NIPS ’22*, Red Hook, NY, USA. Curran Associates Inc.
- Ari Holtzman, Jan Buys, Li Du, Maxwell Forbes, and Yejin Choi. 2020. The curious case of neural text degeneration. In *International Conference on Learning Representations*.
- Daphne Ippolito, Reno Kriz, João Sedoc, Maria Kustikova, and Chris Callison-Burch. 2019. Comparison of diverse decoding methods from conditional language models. In *Proceedings of the 57th Annual Meeting of the Association for Computational Linguistics*, pages 3752–3762.
- Oliver Jenkinson. 2019. Ergodic optimization in dynamical systems. *Ergodic Theory and Dynamical Systems*, 39(10):2593–2618.
- Clara Meister, Tiago Pimentel, Gian Wiher, and Ryan Cotterell. 2023. Locally typical sampling. *Transactions of the Association for Computational Linguistics*, 11:102–121.
- Clara Meister, Gian Wiher, Tiago Pimentel, and Ryan Cotterell. 2022. On the probability-quality paradox in language generation. In *Proceedings of the 60th Annual Meeting of the Association for Computational Linguistics*, volume 2, pages 36–45. Association for Computational Linguistics.

Moin Nadeem, Tianxing He, Kyunghyun Cho, and James Glass. 2020. A systematic characterization of sampling algorithms for open-ended language generation. In *Proceedings of the 1st Conference of the Asia-Pacific Chapter of the Association for Computational Linguistics and the 10th International Joint Conference on Natural Language Processing*, pages 334–346.

OpenAI. 2022. ChatGPT: Optimizing Language Models for Dialogue. <https://openai.com/blog/chatgpt>.

Rafael Rafailov, Archit Sharma, Eric Mitchell, Stefano Ermon, Christopher D. Manning, and Chelsea Finn. 2024. Direct preference optimization: your language model is secretly a reward model. In *Proceedings of the 37th International Conference on Neural Information Processing Systems, NIPS '23*, Red Hook, NY, USA. Curran Associates Inc.

Hugo Touvron, Louis Martin, Kevin Stone, Peter Albert, Amjad Almahairi, Yasmine Babaei, Nikolay Bashlykov, Soumya Batra, Prajwal Bhargava, Shruti Bhosale, et al. 2023. Llama 2: Open foundation and fine-tuned chat models. *arXiv preprint arXiv:2307.09288*.

Ashish Vaswani, Noam Shazeer, Niki Parmar, Jakob Uszkoreit, Llion Jones, Aidan N. Gomez, Łukasz Kaiser, and Illia Polosukhin. 2017. Attention is all you need. In *Proceedings of the 31st International Conference on Neural Information Processing Systems, NIPS'17*, page 6000–6010, Red Hook, NY, USA. Curran Associates Inc.

Peter Walters. 2000. *An introduction to ergodic theory*, volume 79. Springer Science & Business Media.

Gian Wiher, Clara Meister, and Ryan Cotterell. 2022. On decoding strategies for neural text generators. *Transactions of the Association for Computational Linguistics*, 10:997–1012.

Hugh Zhang, Daniel Duckworth, Daphne Ippolito, and Arvind Neelakantan. 2021. Trading off diversity and quality in natural language generation. In *Proceedings of the Workshop on Human Evaluation of NLP Systems (HumEval)*, pages 25–33.

Wayne Xin Zhao, Kun Zhou, Junyi Li, Tianyi Tang, Xiaolei Wang, Yupeng Hou, Yingqian Min, Beichen Zhang, Junjie Zhang, Zican Dong, Yifan Du, Chen Yang, Yushuo Chen, Zhipeng Chen, Jinhao Jiang, Ruiyang Ren, Yifan Li, Xinyu Tang, Zikang Liu, Peiyu Liu, Jian-Yun Nie, and Ji-Rong Wen. 2024. A survey of large language models. *Preprint*, arXiv:2303.18223.

A Computing Local Normalization Distortion for Nucleus and Temperature Sampling

In equations 2 and 3 we described how to compute the ratio of the local normalization distortions of two strings $y_m \cdots y_T$ and $z_m \cdots z_T$ in the case of top-k sampling.

The case of nucleus sampling is almost identical, we need only replace q_k with q_π in equation 3.

For temperature sampling, we note that $q'_\tau(y_m \cdots y_T | \mathbf{y}_{< \mathbf{m}})$ is not proportional to $p(y_m \cdots y_T | \mathbf{y}_{< \mathbf{m}})$, but to $p^{\frac{1}{\tau}}(y_m \cdots y_T | \mathbf{y}_{< \mathbf{m}})$. Thus, to compute the ratio of the local normalization distortions for two strings $y_m \cdots y_T$ and $z_m \cdots z_T$ in the case of temperature sampling, we replace equation 3 with

$$\frac{q_\tau(y_m \cdots y_T | \mathbf{y}_{< \mathbf{m}})}{p^{\frac{1}{\tau}}(y_m \cdots y_T | \mathbf{y}_{< \mathbf{m}})} \cdot \frac{p^{\frac{1}{\tau}}(z_m \cdots z_T | \mathbf{y}_{< \mathbf{m}})}{q_\tau(z_m \cdots z_T | \mathbf{y}_{< \mathbf{m}})}.$$

B Rejection sampling algorithms

We can sample from q'_k , q'_π and q'_τ using rejection sampling. This remains incredibly computationally intensive, but it is significantly easier than computing the probability of each possible string $w_1 \cdots w_T$ as in equation (1).

In the case of top-k and nucleus sampling, with set of allowed completions $\mathcal{A}_{\mathbf{y}_{< \mathbf{m}}}^*$ given context $\mathbf{y}_{< \mathbf{m}}$, one can sample according to the globally normalized variant of top-k or nucleus as follows:

Step 1: Sample a completion $y_m \cdots y_T$ according to the model probability p .

Step 2: Accept the completion $y_m \cdots y_T$ if it is in the allowed set $\mathcal{A}_{\mathbf{y}_{< \mathbf{m}}}^*$, otherwise reject it and repeat step 1.

In the case of temperature sampling, given context $\mathbf{y}_{< \mathbf{m}}$ one can sample according to a globally normalized variant of temperature sampling as follows:

Step 1: Sample a completion $y_m \cdots y_T$ according to the model probability p .

Step 2: Accept this completion with probability $p(y_m \cdots y_T | \mathbf{y}_{< \mathbf{m}})^{\frac{1}{\tau}-1}$. If the completion is not accepted, return to step 1.

We see that with each attempt to sample according to globally normalized temperature sampling, sample $y_m \cdots y_T$ is generated with probability

$$\begin{aligned} & p(y_m \cdots y_T | \mathbf{y}_{< \mathbf{m}}) \times p(y_m \cdots y_T | \mathbf{y}_{< \mathbf{m}})^{\frac{1}{\tau}-1} \\ &= p(y_m \cdots y_T | \mathbf{y}_{< \mathbf{m}})^{\frac{1}{\tau}}. \end{aligned}$$

C Global Temperature Normalization in Ergodic Theory and Fractal Geometry

We mentioned in section 3.1 that global normalization of measures is the standard method in statistical physics, ergodic theory and fractal geometry. A short explanation of this remark is that globally normalized temperature sampling corresponds to taking the Gibbs-equilibrium measure associated to potential $\log p$ at temperature $\frac{1}{\tau}$. Similarly, when using a truncation sampling algorithm with allowed set \mathcal{A} , globally normalized sampling corresponds to sampling from the Gibbs-equilibrium measure associated to potential $\log p$ on the sequence space defined by \mathcal{A} . For both of these comments, see (Bowen, 2008).

For a more direct example, consider extremely long texts generated by pure sampling from a language model with finite context length L . The ergodic theory of Markov chains tells us that, with high probability, the average value of the log probability of a token from the text (‘time average’) will be close to the space average

$$\int_{\text{contexts}} \int_{v_{<t}} \int_{v \in \mathcal{V}} p(v|v_{<t}) dp(v|v_{<t}) dp(v_{<t}).$$

One might ask what can be said about the set of texts for which the average log probability of tokens takes some different value α . How are typical such texts distributed? How many are there? Such questions are answered through the multifractal analysis of ergodic averages, see for example (Falconer, 2007). Solutions involve globally (rather than locally) normalized temperature sampling.

D Proofs

D.1 Proof of Proposition 3.1

We recall Proposition 3.1, which stated that the limit as temperature tends to zero of locally normalized temperature sampling is greedy decoding, whereas the limit as temperature tends to zero of globally normalized temperature sampling is the distribution achieving globally maximal average log likelihood.

The statement on local temperature sampling has been widely noted. It is merely the statement that for any probability vector (p_1, \dots, p_k) , with a unique value p_i larger than all other values, the vector

$$\left(\frac{p_1^{\frac{1}{\tau}}}{\sum_{j=1}^k p_j^{\frac{1}{\tau}}}, \frac{p_2^{\frac{1}{\tau}}}{\sum_{j=1}^k p_j^{\frac{1}{\tau}}}, \dots, \frac{p_k^{\frac{1}{\tau}}}{\sum_{j=1}^k p_j^{\frac{1}{\tau}}} \right)$$

converges to the unit vector with a 1 in position i as $\tau \rightarrow 0$.

The statement on global temperature sampling is more subtle and is a key result linking ‘zero temperature limits of Gibbs measures’ and ‘ergodic optimization’, see for example (Brémont, 2002; Jenkinson, 2019).

D.2 Proof of Corollary 5.1.

We take Lemma 5.1 and set $X = \mathcal{A}_{\mathbf{y}_{< \mathbf{m}}, k}^*$ to be the set of completions $y_m \cdots y_T$ belonging to the top-k set. Our distribution q_k is a probability measure on this set. Then Lemma 5.1 says that q_k is the unique probability measure maximising the quantity

$$H(\mu) + \sum_{\mathbf{w} \in \mathcal{A}_{\mathbf{y}_{< \mathbf{m}}, k}^*} \mu(\mathbf{w} | \mathbf{y}_{< \mathbf{m}}) \log q_k(\mathbf{w} | \mathbf{y}_{< \mathbf{m}})$$

among probability measures μ on the top-k set $\mathcal{A}_{\mathbf{y}_{< \mathbf{m}}, k}^*$. Note that

$$\begin{aligned} & q_k(\mathbf{w} | \mathbf{y}_{< \mathbf{m}}) \\ &= \prod_{i=0}^{T-m} q_k(w_{m+i} | y_0 \cdots y_m w_{m+1} \cdots w_{m+i-1}) \\ &= \prod_{i=0}^{T-m} \frac{p(w_{m+i} | y_0 \cdots y_m w_{m+1} \cdots w_{m+i-1})}{Z_k(y_0 \cdots y_m w_{m+1} \cdots w_{m+i-1})} \\ &= \frac{p(\mathbf{w} | \mathbf{y}_{< \mathbf{m}})}{\prod_{i=0}^{T-m} Z_k(y_0 \cdots y_m w_{m+1} \cdots w_{m+i-1})} \end{aligned}$$

Taking logs and splitting the formula for $\log q_k(\mathbf{w} | \mathbf{y}_{< \mathbf{m}})$ into two distinct terms gives the result.

D.3 Proofs of Corollaries 5.2, 5.3 and 5.4.

These corollaries follow from Lemma 5.1 in an identical manner to the above proof of Corollary 5.1.

E Supplementary figures

Figure 3 is a companion to Table 1 giving the results of section 6.1 across all quantiles.

F A Comment on Timescales for Normalization

In this article we have discussed two different timescales for renormalizing probabilities which do not sum to one, namely locally renormalizing conditional probabilities at each timestep and globally renormalizing probabilities of strings $w_1 \cdots w_T$ at time T , where T is the length of the string we wish

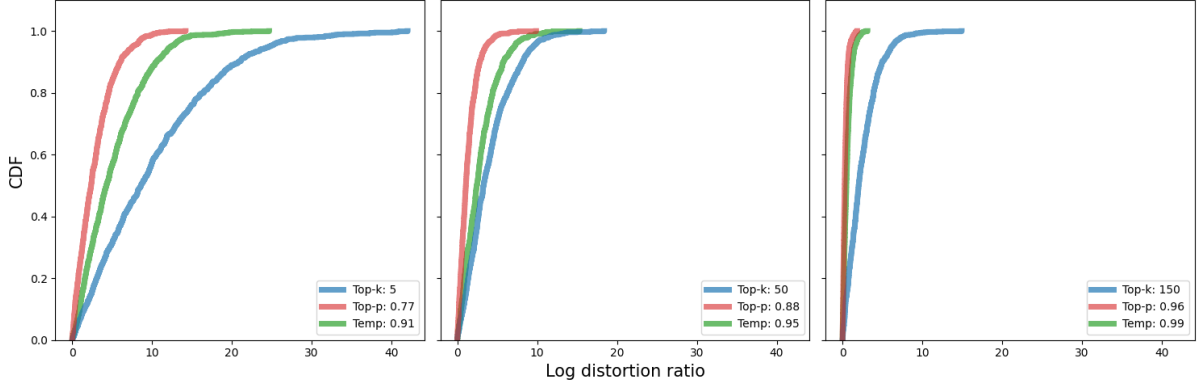


Figure 3: For each graph we generate pairs of texts according to top-k, nucleus or temperature sampling. Parameters for the decoding strategies are tuned so that typical renormalizing quantities Z_k , Z_π and Z_τ are of the same size. We then plot the log of the ratio of the local normalization distortion for the pair of generated texts, and then plot the cumulative distribution function. We see in each case that nucleus sampling produces the smallest local normalization distortion, followed by temperature sampling and top-k sampling.

to generate. There is (at least in theory) a third natural option, which is to renormalize ‘at time infinity’. For example, in the case of temperature sampling at temperature τ , this corresponds to taking the Gibbs measure associated to potential $p^{\frac{1}{\tau}}$ (Bowen, 2008). Precisely, there exists a unique measure q_τ'' on the set \mathcal{A}^∞ such that there exist constants C, P , independent of T , such that

$$\frac{1}{C} \leq \frac{q_\tau''(\{z \in \mathcal{A}^\infty : z_1 \cdots z_T = w_1 \cdots w_T\})}{p^{\frac{1}{\tau}}(w_1 \cdots w_T) \exp(T.P)} \leq C.$$

The constant P , known as the topological pressure, could in theory be explicitly computed as the maximal eigenvalue of a very large matrix.

Normalizing at time infinity has some theoretical appeal, in that it produces a Markov measure whose transition probabilities do not depend on the sequence length T .

G Licenses

We have used Llama 2-7B under the community license agreement, see <https://huggingface.co/meta-llama/Llama-2-7b>. Use for research is consistent with the terms of this license.